

Strain-Engineered Surface Transport in Si(001): Complete Isolation of the Surface State via Tensile Strain

Miao Zhou,¹ Zheng Liu,¹ Zhengfei Wang,¹ Zhaoqiang Bai,² Yuanping Feng,² Max G. Lagally,³ and Feng Liu^{1,*}

¹*Department of Materials Science and Engineering, University of Utah, Salt Lake City, Utah 84112, USA*

²*Department of Physics, National University of Singapore, 117542 Singapore*

³*Department of Materials Science and Engineering, University of Wisconsin, Madison, Wisconsin 53706, USA*

(Received 24 July 2013; published 9 December 2013)

By combining density functional theory, nonequilibrium Green's function formalism and effective-Hamiltonian approaches, we demonstrate strain-engineered surface transport in Si(001), with the complete isolation of the Si surface states from the bulk bands. Our results show that sufficient tensile strain can effectively remove the overlap between the surface valence state and the bulk valence band, because of the drastically different deformation potentials. Isolation of the surface valence state is possible with a tensile strain of $\sim 1.5\%$, a value that is accessible experimentally. Quantum transport simulations of a chemical sensing device based on strained Si(001) surface confirm the dominating surface conductance, giving rise to an enhanced molecular sensitivity. Our results show promise for using strain engineering to further our ability to manipulate surface states for quantum information processing and surface state-based devices.

DOI: [10.1103/PhysRevLett.111.246801](https://doi.org/10.1103/PhysRevLett.111.246801)

PACS numbers: 73.50.-h, 68.60.Bs, 71.20.Mq, 73.20.-r

Silicon in the (001) orientation provides the foundation for modern semiconductor devices. The atomic and electronic structures of the Si(001) surface have been thoroughly investigated and well understood [1,2]. The dangling bonds on the atomically clean Si(001) surface are rebonded in paired asymmetric dimers leading to a $p(2 \times 1)$ reconstruction, which forms surface bonding and antibonding (π and π^*) states with 2D character. At low temperatures, $p(2 \times 2)$ or $c(4 \times 2)$, reconstructions become more stable; these reconstructions modify the surface bands [2]. The unoccupied π^* state of the band structure of the clean Si(001) surface, whose minimum lies below the bulk conduction band minimum, is well separated in energy from bulk bands. In contrast, the occupied surface π state completely overlaps the bulk valence band (VB), with its maximum lying about 0.15 eV below the VB edge at Γ point [3,4].

Engineering surface transport in Si(001) has recently attracted much interest for quantum information processing and surface state-based devices. Local surface conduction has been achieved by atom manipulation using STM [5,6]. In the widely used (001)-oriented silicon-on-insulator system, experiments [7] have shown that global electron transport is possible in very thin clean Si sheet via surface conduction, even in the absence of bulk doping. STM and ultrahigh-vacuum van der Pauw measurement [7,8] suggest that surface transport is enabled by the thermal excitation of electrons from the bulk VB to the surface π^* state. A high surface electron mobility (with density of states of $\sim 10^{15} \text{ cm}^{-2} \text{ eV}^{-1}$) originates from the interaction of surface states with bulk bands [7,8]. However, to achieve surface conduction via holes in addition to electrons (i.e., p -type surface), it is desirable to isolate the surface π band

in energy from the bulk VB, so that electron excitation and transport could occur principally between surface π and π^* states.

Strain engineering of the Si bulk band structure is well understood [9–11] and employed in practice to improve the performance of Si electronics [12,13]. Here, we demonstrate an approach of strain engineering to manipulate Si (001) surface states, relative to the bulk bands, to an unprecedented level. We show that it is possible to achieve pure global surface electron and hole transport without a bulk contribution by applying sufficient tensile strain. We extend strain engineering of Si from bulk to surface by systematically studying the effects of strain on the electronic band structures and transport properties of the Si (001) surface with $p(2 \times 1)$ and $p(2 \times 2)$ reconstructions, using first-principles calculations and quantum transport simulations. Generally, much higher strain can be applied without introducing dislocation in strain-shared multilayer thin films [14–16] or thin films grown on a compliant substrate, such as some silicon-on-insulator systems with Si layer thickness reduced to nanometers [17,18].

Our electronic band structure calculations were performed based on both the screened hybrid functional of Heyd, Scuseria, and Ernzerhof [19] for obtaining accurate bulk and surface band gaps and a generalized gradient approximation (GGA) in Perdew-Burke-Ernzerhof [20] formalism for comparing with quantum transport calculations, as implemented in the VASP code [21]. Results based on using GGA functional calculations are discussed in Fig. S1 in the Supplemental Material [22]. A tight-binding model with effective Hamiltonian was constructed to better understand the surface band modulation induced by strain. Quantum transport simulations were performed using the

nonequilibrium Green's function method coupled with density functional theory (DFT) as implemented in the Atomistix ToolKit package (ATK 11.8) [23,24]. Details of models and computations were presented in the Supplemental Material [22].

In the Si(001) $p(2 \times 1)$ surface, all the asymmetric dimers have the same buckling direction, as shown in Fig. 1(a). Without strain, our calculations using the hybrid functional show that the surface state has an indirect band gap of 0.81 eV, and at Γ point the occupied π band sits ~ 0.147 eV below the VB edge [Fig. 1(c)]. Both the π and π^* bands have a bandwidth around 0.7 eV, in good agreement with previous *GW* calculations [3] and experimental photoemission measurements [4]. In the $p(2 \times 2)$ surface, the dimers alternate their buckling direction along the dimer rows [Fig. 1(b)], so that the interaction between the neighboring dimers leads to splitting of two surface bands into four bands, π_1 , π_2 and π_1^* , π_2^* along high-symmetry lines [see Fig. 1(d)].

Next, we apply biaxial strain to the surface. The buckled dimers remain more stable by 0.16–0.17 eV per unit cell than the unbuckled dimers under 0%–2% tensile strain. Figures 1(e) and 1(f) show the band structures of the $p(2 \times 1)$ and $p(2 \times 2)$ surfaces under a 2% tensile strain, respectively. One sees that the gap between the surface π and π^* bands is decreased and the relative positions of surface bands and that of the bulk bands change significantly for both surfaces. In particular, for the $p(2 \times 1)$ surface, the π band along the ΓJ line, which was buried

in bulk bands without strain, now rises well above the bulk VB, and all the edges of the surface states (π and π^*) lie within the bulk band gap and are completely isolated from bulk bands within an energy window of -0.9 to 0.7 eV. Similar results are obtained in the $p(2 \times 2)$ surface. The π_1 state becomes completely isolated and the π_2 band also rises significantly above the bulk VB. It is also interesting to see that the bandwidth of the surface states in the $p(2 \times 1)$ surface is decreased by tensile strain, while both the occupied (π_1 , π_2) and unoccupied (π_1^* , π_2^*) bands in the $p(2 \times 2)$ surface are split farther apart by strain. These findings indicate that strain can be used as an effective means to tune the surface states against that of the bulk bands in Si(001) surfaces.

The strain-induced isolation of surface states from bulk bands in Si(001) originates from their different response to strain, which can be understood from deformation-potential theory [25,26]. In the past, this theory has been mostly applied to bulk bands; here, we extend it to surface states by defining the surface deformation potential,

$$\Xi = \frac{\partial E_F}{\partial \varepsilon} \pm \frac{1}{2} \frac{\partial E_g}{\partial \varepsilon}, \quad (1)$$

where E_F , E_g , and ε represent Fermi energy, energy gap of the surface states, and the applied strain, respectively. The band-edge energy for the surface states at a particular k point is defined by the Fermi energy and surface gap as $E_{\text{edge}} = E_F \pm \frac{1}{2} E_g$. In Fig. 2, we plot the energies of the upper edge of the surface π state and bulk VB at the Γ point as a function of strain. As Fermi energies of different strained systems are not comparable, we shifted all the energies to vacuum level. From Fig. 2, we derive that the deformation potential of the surface π band is around -0.5 eV while that of bulk VB is -10.1 eV. Such a large

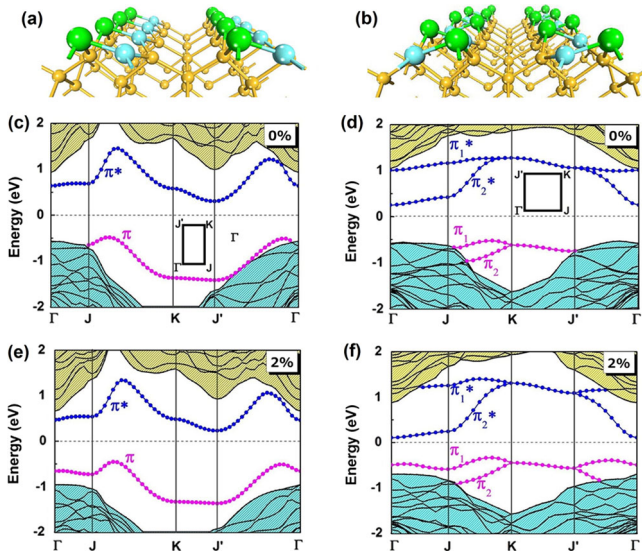


FIG. 1 (color online). (a) Atomic structures of Si(001) surfaces with (a) $p(2 \times 1)$ and (b) $p(2 \times 2)$ reconstruction. (c),(d) Band structures of the $p(2 \times 1)$ and $p(2 \times 2)$ Si(001) surface without strain, respectively. (e),(f) Same as (c) and (d) for the case under a 2% tensile strain. Note that the Si slab has a direct band gap due to folding of two Δ_{\perp} valleys along the surface normal direction into the Γ point [30]. Fermi level is set to zero. Insets in (c) and (d) indicate the surface Brillouin zone.

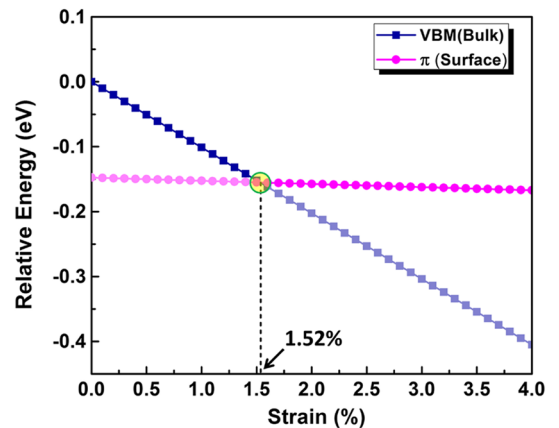


FIG. 2 (color online). Relative energies of the top of the Si(001) $p(2 \times 1)$ surface π state (pink circles) in reference to the Si bulk VB maximum (VBM, blue squares) at the Γ point as a function of strain. The top of the strain-free bulk VB is set to zero of energy. The two energies cross over at a critical strain of 1.52%.

difference in deformation potential is mainly because the surface π state, arising from localized dangling-bond states, is insensitive to strain, while the bulk band, arising from extended Bloch states, is very sensitive to strain. Consequently, with the increasing tensile strain, the bulk VB shifts downward much faster than the surface π state, which can also be seen in Figs. 1(e) and 1(f). Most importantly, there exists a crossover point of energies of the tops of the bulk VB and surface π state at a critical strain of 1.52%: below it, the surface π band is completely buried inside the bulk VB; above it, the surface π band starts to move above the bulk VB. Therefore, we theoretically define a critical tensile strain of 1.5% to begin isolating filled surface states in the Si(001) surface, above which pure surface transport of both electrons and holes becomes possible by tuning the Fermi level above the maximum of the bulk VB.

Microscopically, we may associate the strain-induced modulation of surface states to strain-induced change of

surface atomic structure, in particular, the dimer buckling angle, in terms of Jahn-Teller distortion (see Section III in the Supplemental Material [22]). Based on the structural analysis, we constructed an effective tight-binding Hamiltonian to model the 2D electronic structures of the Si(001) surface dimers and to analyze qualitatively their strain dependence, in terms of surface gap, bandwidth, and band splitting. The schematic atomic models of the $p(2 \times 1)$ and $p(2 \times 2)$ surface dimers are shown in Figs. S3 and S4 of the Supplemental Material [22]. The Hamiltonian for the $p(2 \times 1)$ surface dimers is expressed as

$$H = \begin{pmatrix} \varepsilon_u + t_1(e^{-ik_y} + e^{ik_y}) & t_0e^{-ik_x} + t_2e^{ik_x} \\ t_0e^{ik_x} + t_2e^{-ik_x} & \varepsilon_d + t'_1(e^{-ik_y} + e^{ik_y}) \end{pmatrix}, \quad (2)$$

and that for the $p(2 \times 2)$ is

$$H = \begin{pmatrix} \varepsilon_u & t_0e^{ik_x} + t_2e^{-ik_x} & 0 & t_1(e^{-ik_y} + e^{ik_y}) \\ t_0e^{-ik_x} + t_2e^{ik_x} & \varepsilon_d & t_1(e^{-ik_y} + e^{ik_y}) & 0 \\ 0 & t_1(e^{ik_y} + e^{-ik_y}) & \varepsilon_u & t_0e^{-ik_x} + t_2e^{ik_x} \\ t_1(e^{-ik_y} + e^{ik_y}) & 0 & t_0e^{ik_x} + t_2e^{-ik_x} & \varepsilon_d \end{pmatrix}, \quad (3)$$

where ε_u (ε_d) denotes the on-site energy of the upper (lower) atom in a dimer, t_0 is the hopping energy between these two atoms, t_1 (t'_1) and t_2 are the hopping energies between two nearest atoms in two neighboring dimers along and perpendicular to the dimer row, respectively. Calculations show that the buckling angle, which defines the coupling strength (t_0) between the two atoms within a dimer, is crucial to determine the surface gap. With increasing tensile strain, the buckling angle decreases so that t_0 decreases, leading to a reduction of surface gap in both $p(2 \times 1)$ and $p(2 \times 2)$ surfaces (Tables S-I and S-II in the Supplemental Material [22]). The bandwidth of the $p(2 \times 1)$ surface bands and the band splitting of the $p(2 \times 2)$ surface bands are found to depend on the coupling strength (t_1 , t'_1) between two Si atoms in the neighboring dimers along the dimer row direction. In the tensile strained $p(2 \times 1)$ surface, the interaction t_1 between two neighboring dimers decreases due to the increased dimer-dimer distance, hence, narrowing the surface bandwidth (Table S-III [22]), while in the $p(2 \times 2)$ surface, tensile strain increases t_1 because, with a smaller buckling angle, the neighboring dimers become more “parallel” to each other, resulting in stronger interaction, hence, increasing the surface band splitting (Table S-IV [22]). All of the above analysis agrees well with the DFT calculations.

The above band calculation results indicate the possibility of complete isolation of surface transport for building pure surface state-based devices. Even if there is still

partial overlap between the π surface state and the bulk VB, as long as one can tune the Fermi level above the maximum of the bulk VB, one can achieve isolation of surface transport. This cannot be done without strain because the π surface state is completely buried in the bulk VB. Sufficient tensile strain allows us to separate surface transport from bulk transport, so as to study the mobility difference between surface and bulk carriers, interaction of surface states with bulk bands, etc. Temperature dependence measurements might see localization effects of the surface state (something that does not happen with bulk states). It is important to point out that the 1.5% critical strain required for isolation of the surface state is readily achievable in experiments by growing ultrathin Si films (10–50 nm) on “virtual” SiGe substrate [12,13] or fully elastically relaxed SiGe nanomembranes [14], with the amount of strain controlled by the Ge concentration. In addition, large local tensile strain may be induced by growth of SiGe nanostressors on Si nanomembrane or nanowire [27].

We have carried out quantum transport calculations to illustrate this point. In Fig. 3(a), we show the schematic diagram of a proposed surface-state device using a tensilely strained Si(001) surface. A backgate voltage can be applied to tune the energy window for surface conductance. As a model study, we assume the Si(001) have a $p(2 \times 1)$ reconstruction. Equilibrium conductance spectra for the Si(001) surface without strain and with 2% tensile

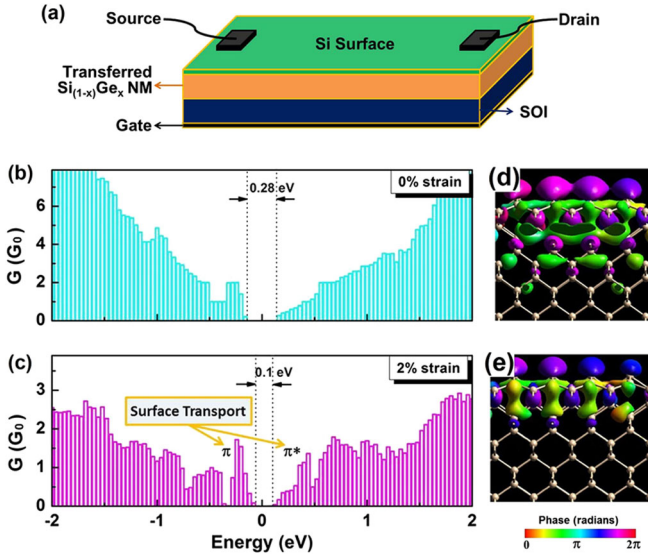


FIG. 3 (color online). (a) Schematic view of experimental setup to measure the SiNM surface conductance. (b),(c) Conductance spectra for a Si(001) $p(2 \times 1)$ surface without strain and with a 2% tensile strain, respectively. Transport gaps are indicated, and for the strained case, surface transport due to π and π^* bands is also indicated. (d),(e) Conductance eigenchannel corresponding to (b) and (c), respectively, at the Γ point evaluated at $E = -0.2$ eV.

strain are presented in Figs. 3(b) and 3(c), respectively. It is found that the transport gap for the $p(2 \times 1)$ Si surface without strain is about 0.28 eV. We note that this gap is smaller than the real gap as shown in Fig. 1, because the hybrid functional is not available for transport calculations in current ATK package. Thus, for comparison, we also performed band structure calculation using the GGA functional, which produces a similarly underestimated band gap (see Fig. S1 in Supplemental Material [22]). Without strain, the conductance spectra show indistinguishable contributions from the surface and bulk states, because they are mixed [Fig. 3(b)]. Under 2% tensile strain, the transport gap significantly reduces to around 0.1 eV. Most strikingly, the surface π band conductance is totally isolated from the bulk, and the π^* band also shows up evidently with little overlap from bulk contribution [Fig. 3(c)].

Another interesting finding is the magnitude of surface conductance compared to bulk conductance in response to strain. In the energy range from -2 to 2 eV, the bulk conductance drops by a factor of 3 by applying a tensile strain; in contrast, the surface conductance remains $2G_0$ (with quantum conductance $G_0 = 2e^2/h$). The origin of this difference can be understood by considering the deformation potential of the “deeper” energy bands within this energy range that contribute to the bulk conductance. Referring back to Fig. 1(e), there is a dramatic downshift of bulk bands upon tensile strain so that the bulk states within this energy window become much less, leading to a

large reduction of bulk conductance. However, the surface bands are hardly affected because of its much smaller deformation potential. In this sense, “intrinsic” surface conductance, i.e., conductance purely arising from surface states, can be directly measured by fine-tuning the gate voltage to an appropriate value, so as to minimize the bulk conductance using a typical experimental setup such as the van der Pauw measurement [8].

Further support for the isolation of surface-state conductance is provided by plotting the conductance eigenchannel at the Γ point with $E = -0.2$ eV, at 0% and 2% tensile strain, as shown in Figs. 3(d) and 3(e), respectively. Clearly, without strain, the conductance eigenchannel is spread over the Si(001) film and extends down to the 8th atomic layer [Fig. 3(d)]. Correspondingly, the incoming wave function will interfere with the bulk wave functions, and is prone to be scattered by the underlying defects (vacancies, impurities, dislocations, etc.) if they are present. In contrast, under tensile strain, the eigenchannel is localized in the top region of the surface within the top four layers [Fig. 3(e)]. Therefore, charge carriers can travel for a longer distance without being scattered by bulk states. Consequently, leakage current can be efficiently reduced.

The surface-state transport is also expected to be quite sensitive to surface adsorption, useful for chemical sensing. In particular, the isolated surface π and π^* states associated with the surface of strained Si(001) will likely increase the sensitivity towards gas molecule surface adsorption, relative to the unstrained surface whose surface bands overlap with the bulk bands. To prove this hypothesis, we have examined a model gas sensing device (see Fig. S5 [22]) based on the strained Si surface, and a typical small gas molecule, NO_2 , was chosen as an example to illustrate the strain-enhanced surface sensitivity. Transport calculations were performed for a six-layer Si(001) $p(2 \times 1)$ surface without and with a 2% tensile strain upon NO_2 adsorption. Various adsorption geometries are considered, the I - V curves are shown in Fig. 4(a) for the most stable configurations (see Fig. S6 [22]), under the bias within the

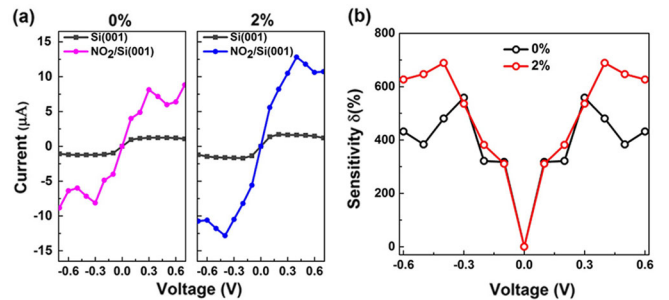


FIG. 4 (color online). (a) The I - V curve of a six-layer Si(001) $p(2 \times 1)$ surface with NO_2 adsorption without strain (left) and with a 2% tensile strain (right), in comparison with the I - V curve of the clean Si surface. (b) The device sensitivity towards NO_2 adsorption as a function of bias voltage.

energy window of the Si bulk band gap, where the isolated surface bands reside. It is found that the current for the Si(001) $p(2 \times 1)$ surface changes significantly upon adsorption of the NO₂ molecule, in both strain-free (pink versus gray) and strained (blue versus gray) surfaces [Fig. 4(a)], indicating high sensitivity of a surface-state chemical sensing device. The increase of current is further magnified for the strained surface, which translates into additional strain-induced enhancement of device sensitivity. In Fig. 4(b), we plot the sensitivity of the proposed device towards NO₂ under different bias voltages. Here, the sensitivity (δ) is defined as $\delta = (I_{\text{ad}} - I_0)/I_0 \times 100\%$, with I_{ad} (I_0) being the current with (without) molecular adsorption. We found that the sensitivity of the strained Si surface towards NO₂ adsorption increases by 50% when the applied bias voltage is larger than 0.4 V, relative to the strain-free surface.

To conclude, based on DFT band structure and quantum transport calculations, we demonstrate that sufficient tensile strain can isolate the Si(001) surface states from the bulk bands. We identify a critical strain of $\sim 1.5\%$ for the onset of surface-state isolation, which is readily achievable in experiments [12–14]. The strain-engineered surface-state isolation is found to be very robust against surface defects [22], such as the type-C defect formed on Si(001) upon water adsorption [28,29], and is useful for ultrasensitive chemical sensing applications. We believe the fundamental principle underlying the use of strain engineering to modify relative positions of bulk and surface bands is generally applicable to surfaces of other materials having appropriate surface states.

This research was supported by DOE (Grant No. DE-FG02-04ER46148). We thank DOE-NERSC, CHPC at University of Utah, and CCSE at National University of Singapore for providing the computing resources.

*fliu@eng.utah.edu

- [1] F. Liu, M. Hohage, and M. G. Lagally, in *Structure of Surfaces and Interfaces*, Encyclopedia of Applied Physics, Supplemental Volume, edited by H. Immergut and G. Trigg (Wiley-VCH Verlag GmbH, London, 1999), pp. 321–352.
- [2] G. P. Srivastava, *Theoretical Modelling of Semiconductor Surfaces* (World Scientific, Singapore, 1999).
- [3] M. Rohlffing, P. Krüger, and J. Pollmann, *Phys. Rev. B* **52**, 1905 (1995).
- [4] C. Kentsch, M. Kutschera, M. Weinelt, T. Fauster, and M. Rohlffing, *Phys. Rev. B* **65**, 035323 (2001).
- [5] B. Weber, S. Mahapatra, H. Ryu, S. Lee, A. Fuhrer, T. C. G. Reusch, D. L. Thompson, W. C. T. Lee, G. Klimeck, L. C. L. Hollenberg, and M. Y. Simmons, *Science* **335**, 64 (2012).
- [6] S. R. Schofield, P. Studer, C. F. Hirjibehedin, N. J. Curson, G. Aepli, and D. Bowler, *Nat. Commun.* **4**, 1649 (2013).
- [7] P. P. Zhang, E. Tevaarwerk, B. N. Park, D. E. Savage, G. K. Celler, I. Knezevic, P. G. Evans, M. A. Eriksson, and M. G. Lagally, *Nature (London)* **439**, 703 (2006).
- [8] W. Peng, Z. Aksamija, S. A. Scott, J. J. Endres, D. E. Savage, I. Knezevic, M. A. Eriksson, and M. G. Lagally, *Nat. Commun.* **4**, 1339 (2013).
- [9] D. Yu, Y. Zhang, and F. Liu, *Phys. Rev. B* **78**, 245204 (2008).
- [10] M. Chu, Y. Sun, U. Aghoram, and S. E. Thompson, *Annu. Rev. Mater. Res.* **39**, 203 (2009).
- [11] Z. Liu, J. Wu, W. H. Duan, M. G. Lagally, and F. Liu, *Phys. Rev. Lett.* **105**, 016802 (2010).
- [12] C. W. Leitz, M. T. Currie, M. L. Lee, Z.-Y. Cheng, D. A. Antoniadis, and E. A. Fitzgerald, *J. Appl. Phys.* **92**, 3745 (2002).
- [13] M. L. Lee, E. A. Fitzgerald, M. T. Bulsara, M. T. Currie, and A. Lochtefeld, *J. Appl. Phys.* **97**, 011101 (2005).
- [14] D. M. Paskiewicz, B. Tanto, D. E. Savage, and M. G. Lagally, *ACS Nano* **5**, 5814 (2011).
- [15] M. M. Roberts, L. J. Klein, D. E. Savage, K. A. Slinker, M. Friesen, G. K. Celler, M. A. Eriksson, and M. G. Lagally, *Nat. Mater.* **5**, 388 (2006).
- [16] M. H. Huang, P. Rugheimer, M. G. Lagally, and F. Liu, *Phys. Rev. B* **72**, 085450 (2005).
- [17] F. Liu, P. Rugheimer, E. Mateeva, D. E. Savage, and M. G. Lagally, *Nature (London)* **416**, 498 (2002).
- [18] F. Liu, M. Huang, P. P. Rugheimer, D. E. Savage, and M. G. Lagally, *Phys. Rev. Lett.* **89**, 136101 (2002).
- [19] J. Heyd, G. E. Scuseria, and M. Ernzerhof, *J. Chem. Phys.* **118**, 8207 (2003); **124**, 219906 (2006).
- [20] J. P. Perdew, K. Burke, and M. Ernzerhof, *Phys. Rev. Lett.* **77**, 3865 (1996).
- [21] G. Kresse and J. Hafner, *Phys. Rev. B* **47**, 558 (1993).
- [22] See Supplemental Material at <http://link.aps.org/supplemental/10.1103/PhysRevLett.111.246801> for computational details, band structures calculated using GGA functional, Jahn-Teller distortion picture of $p(2 \times 1)$ surface, tight-binding models for $p(2 \times 1)$ and $p(2 \times 2)$ surface dimers, the proposed ultrasensitive chemical sensing device, and the discussion of strain effects on Si(001) surface with defects.
- [23] M. Brandbyge, J. L. Mozos, P. Ordejón, J. Taylor, and K. Stokbro, *Phys. Rev. B* **65**, 165401 (2002).
- [24] J. Taylor, H. Guo, and J. Wang, *Phys. Rev. B* **63**, 121104 (2001).
- [25] C. Herring and E. Vogt, *Phys. Rev.* **101**, 944 (1956).
- [26] H. Hu, M. Liu, Z. F. Wang, J. Zhu, D. Wu, H. Ding, Z. Liu, and F. Liu, *Phys. Rev. Lett.* **109**, 055501 (2012).
- [27] M. Huang, C. S. Ritz, B. Novakovic, D. Yu, Y. Zhang, F. Flack, D. E. Savage, P. G. Evans, I. Knezevic, F. Liu, and M. G. Lagally, *ACS Nano* **3**, 721 (2009).
- [28] S. Y. Yu, H. Kim, and J. Y. Koo, *Phys. Rev. Lett.* **100**, 036107 (2008).
- [29] S. A. Scott, W. Peng, A. M. Kiefer, H. Q. Jiang, I. Knezevic, D. E. Savage, M. A. Eriksson, and M. G. Lagally, *ACS Nano* **3**, 1683 (2009).
- [30] T. B. Boykin, G. Klimeck, M. A. Eriksson, M. Friesen, S. N. Coppersmith, P. von Allmen, F. Oyafuso, and S. Lee, *Appl. Phys. Lett.* **84**, 115 (2004).